M. I. Goodisman

M. L. G. Oldfield

Department of Engineering Science,
Oxford University,
Oxford, United Kingdom

R. C. Kingcombe
Royal Aerospace Establishment,
Pyestock, Farnborough, United Kingdom

T. V. Jones

R. W. Ainsworth

Department of Engineering Science,
Oxford University,
Oxford, United Kingdom

A. J. Brooks
Royal Aerospace Establishment,
Pyestock, Farnborough, United Kingdom

An Axial Turbobrake

The "Axial Turbobrake" (patent applied for) is a novel turbomachine that can be used to absorb power generated by test turbines. Unlike a compressor, there is no pressure recovery through the turbobrake. This simplifies the aerodynamic design and enables high-stage loadings to be achieved. The blades used have high-turning two-dimensional profiles. This paper describes a single-stage axial turbobrake, which is driven by the exhaust gas of the test turbine and is isolated from the turbine by a choked throat. In this configuration no fast-acting controls are necessary as the turbobrake operates automatically with the turbine flow. Tests on a 0.17 scale model show that the performance is close to that predicted by a simple two-dimensional theory, and demonstrate that the turbobrake power absorption can be controlled and hence matched to that typically produced by the first stage of a modern highly loaded transonic turbine. A full-size axial turbobrake will be used in a short-duration rotating turbine experiment in an Isentropic Light Piston Tunnel at RAE Pyestock.

Introduction

Research into heat transfer in modern gas turbines has led to the construction of rotating turbine facilities that closely model the real engine environment. Short-duration facilities that model the gas/wall/coolant temperature ratios rather than the actual high turbine temperatures are cost effective and are easy to instrument due to their low temperature.

The designer of a short-duration rotating turbine facility has the choice of either allowing the turbine to accelerate during a run or of absorbing the rotor power to hold its speed constant. Tunnels such as the Isentropic Light Piston Tunnel at Oxford University (Ainsworth et al., 1988) and the shock tube rotor at Calspan (Dunn et al., 1984) have been designed without a turbine brake, greatly simplifying their design. At MIT an eddy current brake was used (Epstein et al., 1984).

Brake design is a challenging problem for short-duration facilities, but results in a tunnel potentially capable of more productive and accurate testing. The desired blade speed is maintained during a run, enabling instrumentation traversing. Also, multiple measurements can be taken during a run and averaged without errors due to changing blade speed.

There are also safety issues. The maximum rotor overspeed permitted will limit the run time if there is no brake.

This paper describes a new type of turbomachine, the axial turbobrake. It was designed to absorb the power of the first stage of a modern transonic gas turbine to be tested in the Isentropic Light Piston Cascade (ILPC), a short-duration facility at RAE Pyestock in England (Brooks et al., 1985). This single-stage device is driven by the exhaust gas of the test turbine and is isolated from it by a choked throat. Tests on a 0.17 scale model axial turbobrake are described. These agree surprisingly well with a simple two-dimensional theory. The turbobrake is seen to have applications to both continuous and short-duration facilities.

Braking Requirement

The ILPC rotating section will include a turbine rotor and brake connected to the same shaft (Fig. 1).

The brake must fulfill the following requirements:

(*i*) It must absorb the turbine power for all turbine test conditions.

(*ii*) It must be fail safe.

(*iii*) Its power must be adjustable in order to match the turbine power over the test speed range.

(*iv*) It must not restrict or disturb the turbine flow.

The turbine test conditions are shown in Table 1 and the corresponding ILPC operating conditions are shown in Table 2.

Contributed by the International Gas Turbine Institute and presented at the 36th International Gas Turbine and Aeroengine Congress and Exposition, Orlando, Florida, June 3–6, 1991. Manuscript received at ASME Headquarters January 18, 1991. Paper No. 91-GT-1. Associate Editor: L. A. Riekert.

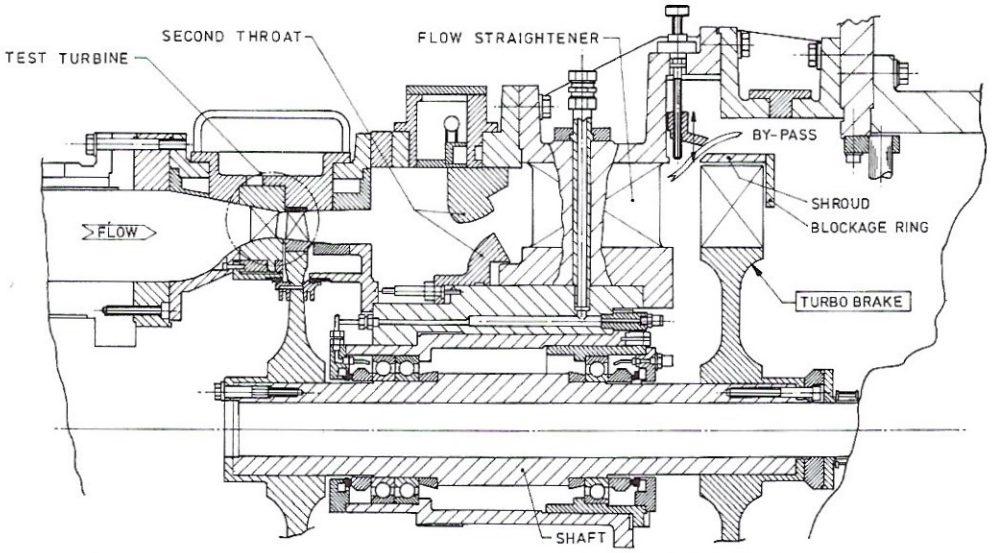

Fig. 1 Proposed axial turbobrake mounted on test turbine in ILPC tunnel at RAE Pyestock

Table 1 Turbine test conditions (total conditions at NGV inlet)

	At design	Off design
Stage loading, $\Delta h_{ot}/U_t^2$	1.53	90–110 percent
Blade Mach number, U_t/a_{01t}	0.60	90–110 percent
Reynolds number, $\dot{m}/\mu_{01t}D_t$	1.38×10^6	50–200 percent
Flow coefficient, $\dot{m}\sqrt{(RT_{01t})}/p_{01t}D_t^2$	0.0483	
NGV gas/wall temperature ratio	1.76	

Table 2 ILPC tunnel design operating conditions

Test time	400 ms
Fluid	Air
Power, P	2.30 MW
Rotational speed	9500 rpm
Mass flow rate, $\dot{m}$	20.7 kg/s
Rotor hub/tip radii	0.252/0.296 m
Total pressure inlet/exit, p_o	5.44/2.10 bar
Total temperature inlet/exit, T_o	508/394 K
Total viscosity inlet/exit, μ_o	$27.0\times10^{-6}/22.6\times10^{-6}$ Pas
Exit absolute swirl angle	22 deg
Mach No. at exit	0.46

Possible Braking Systems

There exist today many braking devices, or dynamometers, capable of absorbing the power produced by a test turbine stage. The cold flow turbine test rig of Westinghouse Canada Inc. (Gosling, 1984) tests turbines up to 7000 rpm. It used a Froude hydraulic dynamometer rated at 600 kW to absorb the power produced by a turbine of tip diameter 686 mm. Hydraulic dynamometers are widely used, heat generated being easily removed by ensuring a steady flow of working fluid through the device. The electric eddy current brake of the DFVLR-AVA rotating cascade rig at Gottingen (Heinemann, 1979) is rated at 500 kW, absorbing the power produced by a 520-mm test wheel rotating up to 15,000 rpm. A full range of dynamometer types is given by Judge (1955).

These brakes, however, have not been developed for use on short-duration facilities. In these facilities, the turbine rotor is spun up to its test speed before the test gas is released. The brake must turn on at the instant the test gas reaches the turbine. Failure to do so at the correct time would result in the wrong test speed or even the turbine accelerating to its burst speed with potentially catastrophic consequences.

The MIT blowdown turbine facility (Epstein et al., 1984, 1985) is a short-duration facility that uses a specially designed eddy current brake to absorb the turbine stage power (1.078 MW) at its design speed of 6190 rpm. At present, this is the only short-duration facility with a brake. The facility has a run time of 400 ms, testing a 500-mm-dia. turbine stage using an Argon/Freon test gas. This test gas permits a much slower rotor angular velocity than for air. Consequently, even if the brake fails, the rotor cannot accelerate to its burst speed.

A number of braking systems were considered for the ILPC (Schultz, 1983). A sufficiently large flywheel was found to be too massive. A disk brake was found to be feasible. However, both it and an eddy current brake require fast-acting controls to activate and deactivate them. Failure of the control system would lead to catastrophic overspeed. For this reason, attention turned to use of an air brake.

An air brake driven by the turbine exhaust gas would be fail safe. No fast-acting controls would be needed, the brake being activated and deactivated by the turbine flow. Pressure

Nomenclature

a = speed of sound
I = moment of inertia
C_P, C_v = specific heat at const. pressure, volume
D = mean rotor blade diameter
Δh_o = change in total enthalpy per unit mass
M = Mach number
NGV = nozzle guide vane
$\dot{m}$ = mass flow rate
N = rpm
P = power
p = pressure
R = gas constant
r = radius
T = temperature
U = mean blade velocity
v = fluid velocity
α = swirl angle
γ = ratio of specific heats
μ_o = total viscosity
ϕ = flow coefficient = $[\dot{m}\sqrt{(RT_{01})}]/[p_{01}D^2]$
ψ = stage loading = $\Delta h_o/U^2$

Subscripts

b = brake
r = relative to rotor
t = turbine
0 = total
1 = at rotor inlet
2 = at rotor exit
* = at throat

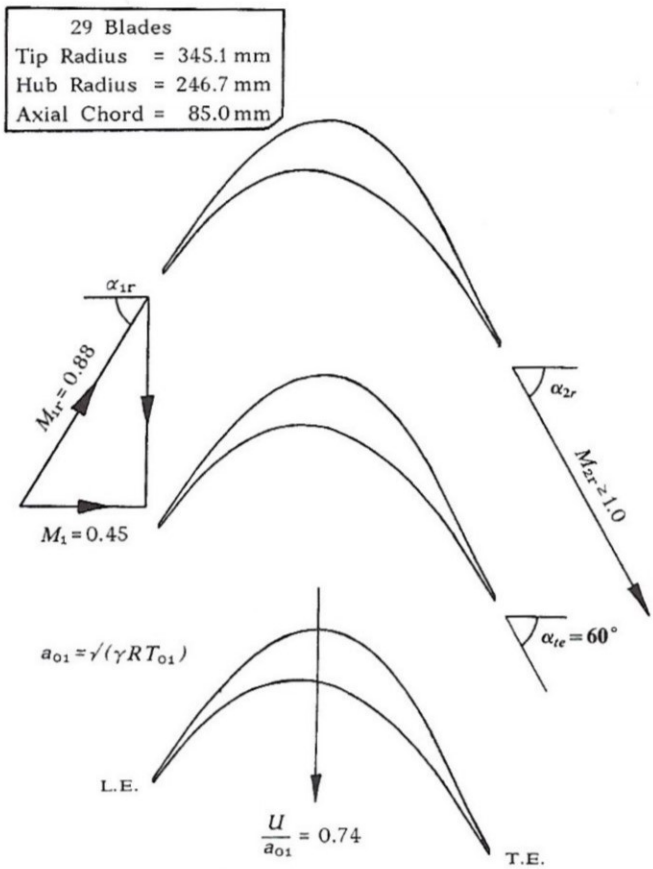

Fig. 2 Midheight section of axial turbobrake blades

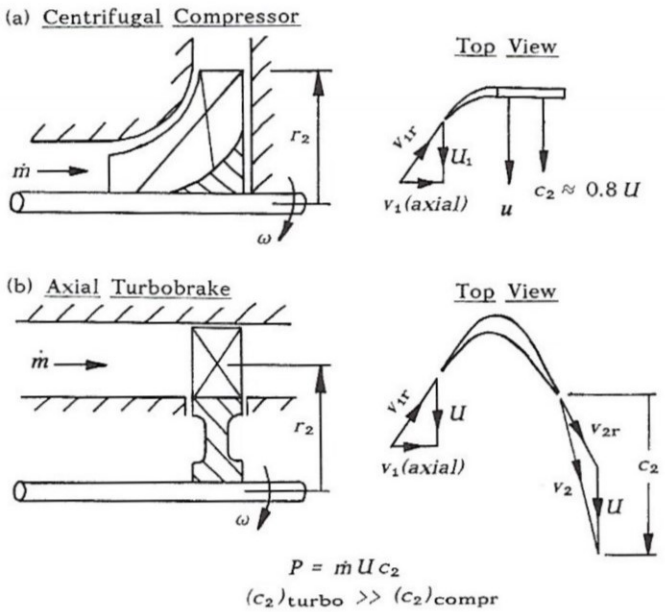

Fig. 3 Comparison of exit whirl velocity c_2 produced by (*a*) centrifugal compressor and (*b*) axial turbobrake of similar diameter. The power absorbed, $P=\dot{m}Uc_2$, is far greater for the turbobrake.

fluctuations from the brake could be isolated from the turbine test section by a choked throat (the second throat in Fig. 1) between the turbine and air brake. This throat would also be used to set the turbine back pressure. An additional advantage of an air brake is that the heat generated during braking is carried away by the flow, and so the brake needs no cooling.

Existing compressor technology was considered. For simplicity, a single-stage device was preferred. A centrifugal compressor stage absorbs more power than an axial compressor stage but is still less powerful than a transonic turbine stage of similar diameter and mass flow. Power scales with the square of the compressor diameter, but the brake power required leads to an excessively large centrifugal compressor. Epstein et al. (1985) came to a similar conclusion.

A successful air dynamometer, using a double-sided radial outflow turbine, has been developed by Foor and Jansen (1984). For the power absorption required by the present study, a radial outflow turbine would require a large-diameter exit flow collector, and the cantilevered blading presents stress problems. For these reasons an axial flow geometry is preferred.

Theory of Axial Turbobrake

The axial turbobrake concept comes directly from Euler's pump equation:

$$P/\dot{m} = \Delta h_o = U_2 c_2 - U_1 c_1$$

This shows that the power P transferred by a rotor to a fluid of mass flow rate $\dot{m}$ can be maximized by achieving the maximum change in fluid tangential velocity (or swirl) c coupled with the maximum blade speed, U. This criterion is different from that of a compressor, whose purpose is the efficient compression of gas. With the requirement of compression removed, a new turbomachine, optimized for power adsorption, was designed and termed the axial turbobrake (referred to also as just turbobrake).

The design philosophy adopted was to choose an axial flow device and use a blade profile (Fig. 2) that added as much whirl velocity as possible to the incoming axial flow. The lack of an NGV, together with the high blade speeds planned, gives a high blade relative inlet Mach number (typically $M_{1r}=0.88$) and this in turn dictates the use of a steeply inclined, sharp leading edge. The flow is then turned sharply and leaves the passage supersonically in the direction of blade rotation with about 60 deg swirl, exhausting into a low-pressure downstream region.

Figure 3 compares the turbobrake velocity triangles to those of the centrifugal compressor. It shows the larger tangential velocity changes in the turbobrake for a given blade speed.

In the axial turbobrake, unlike an axial compressor, there exists a net negative pressure difference across the rotor. No pressure recovery is required, so there is no overall diffusion through the rotor and no need for diffusing nozzle guide vanes downstream of the rotor. This negative axial pressure gradient greatly simplifies the design, allowing high blade curvature without catastrophic stall. This should also reduce the possibility of surge.

As high efficiency is not required, flow separations within the blade passage can be tolerated, provided that the acceleration at exit re-attaches the flow and that the effective throat area is not reduced to an extent whereby the turbobrake upstream pressure is raised enough to unchoke the upstream isolating throat.

The profile shown in Fig. 2 was designed by Gareth Horton at RAE Pyestock. For ease of manufacture, a two-dimensional blade profile, with constant tip and hub radii, was chosen.

Although an axial turbobrake can have inlet guide vanes to add inlet swirl, these are not necessary. This study concentrates on the simpler design with axial inlet flow.

With axial flow at the turbobrake inlet and constant blade tip and hub radii, Euler's turbine equation becomes

$$\Delta h_o = U c_2 = U(U + v_{2r} \sin \alpha_{2r}).$$

Assuming perfect gas, adiabatic flow, the brake performance can be nondimensionalized by expressing the stage loading ψ in terms of the blade rotational Mach number U/a_o (equivalent to $N/\sqrt{T}$), relative exit Mach number M_{2r}, and relative exit angle α_{2r}:

$$v_{2r} = M_{2r} a_{2r} = M_{2r} a_{01} \sqrt{\left(\frac{T_{or}}{T_{01}} \frac{T_{2r}}{T_{or}}\right)}.$$

The energy equation for adiabatic flow gives

$$\frac{T_{or}}{T_{2r}} = 1 + \frac{\gamma - 1}{2} M_{2r}^2$$

Equating static enthalpies at the blade entry,

$$h_{01} - \frac{1}{2} v_1^2 = h_{or} - \frac{1}{2} v_{1r}^2,$$

or

$$C_p T_{01} - \frac{1}{2} v_1^2 = C_p T_{0r} - \frac{1}{2}(v_1^2 + U^2).$$

Noting that $C_p = \gamma R/(\gamma - 1)$ and that $a_{01} = \sqrt{(\gamma R T_{01})}$, we get

$$\frac{T_{or}}{T_{01}} = 1 + \frac{\gamma - 1}{2}\left(\frac{U}{a_{01}}\right)^2.$$

Combining the above four equations gives

$$\psi = \frac{\Delta h_o}{U^2} = 1 + \frac{M_{2r} \sin \alpha_{2r}}{\left(\frac{U}{a_{01}}\right)} \left(\frac{1 + \frac{\gamma - 1}{2}\left(\frac{U}{a_{01}}\right)^2}{1 + \frac{\gamma - 1}{2} M_{2r}^2} \right)^{1/2} \quad (1)$$

Equation (1) clearly shows that ψ can be maximized by using large values of α_{2r} and M_{2r}. In practice, since sin(60 deg) = 0.866, relative exit angles of 60–70 deg are sufficient. A large vacuum vessel is used to maintain the downstream pressure near to vacuum during the run up and this ensures that, during test time, $M_{2r} > 1.0$.

For design purposes, the conservative assumption was that $M_{2r} = 1.0$. Then, for air with $\gamma = 1.4$, and at a typical $U/a_{01} = 0.74$, Eq. (1) gives $\psi = 2.13$ for $\alpha_{2r} = 60$ deg, increasing at 2.22 at 70 deg. This is more than double that of a centrifugal compressor of the same diameter, where $\sin \alpha_{2r} \approx 0$, giving $\psi \approx 1.0$.

Since the power absorbed, $P = \dot{m} \Delta h_o = \dot{m} \psi U^2$, it follows that P can be increased, for a given $\dot{m}$, by increasing the turbobrake diameter, and hence U, and still keep within mechanical and structural limits.

Matching Turbobrake to Turbine

The turbine stage loading $\psi_t = \Delta h_{ot}/U_t^2$ is based on the midheight turbine blade speed U_t. Although the turbobrake is mounted on the same shaft (Fig. 1), and rotates at the same angular velocity, it has a different midheight diameter D_b and hence a different midheight blade speed, $U_b = U_t(D_b/D_t)$. The turbobrake has to absorb the turbine Δh_o, and so has a required turbobrake stage loading,

$$\psi_b = \Delta h_{ot}/U_b^2 \quad (2)$$

The turbine cools the flow through it and hence reduces the sound speed a_{01b} upstream of the turbobrake. This changes the rotational Mach number U_b/a_{01b}:

$$\left(\frac{U_b}{a_{01b}}\right) = \left(\frac{U_t}{a_{01t}}\right)\left(\frac{U_b}{U_t}\right)\left(\frac{a_{01t}}{a_{01b}}\right)$$

As $\Delta h_{ot} = C_p(T_{01t} - T_{01b})$, (a_{01t}/a_{01b}) can be found. (U_b/U_t) depends only on the geometry of the turbine and brake, and so the required nondimensional turbobrake speed is given by

$$\left(\frac{U_b}{a_{01b}}\right) = \left(\frac{U_b}{U_t}\right)\left(\frac{U_t}{a_{01t}}\right)\left[1 - (\gamma - 1)\psi_t\left(\frac{U_t}{a_{01t}}\right)^2\right]^{-1/2} \quad (3)$$

Table 3 Turbobrake at design conditions

Required stage loading (Eq. (2)), $\Delta h_{0t}/U_b^2$	1.32
Theoretical stage loading (Eq. (1)), $\Delta h_{0b}/U_b^2$	2.13
Blade Mach number, U_b/a_{01b} (Eq. (3))	0.74
Number of blades	29
Fluid	Air
Required power, P	2.3 MW
Maximum power	3.8 MW
Rotational speed	9500 rpm
Mass flow rate, $\dot{m}$	20.7 kg/s
Blade axial chord	85 mm
Rotor hub/tip radii	246.7/345.1 mm
Total temperature inlet, T_{01b}	394 K
Total viscosity inlet, μ_{01}	22.6×10^{-6} Pas
Relative exit swirl angle, α_{2r}	60 deg
Relative exit Mach number, M_{2r}	>1.0

Turbobrake Design

Initially a 70 deg exit flow turbobrake was designed and model tested. It worked, but proved to have insufficient throat area. The resulting pressure upstream of the brake permitted the isolating second throat between the turbine and the brake (Fig. 1) to unchoke.

This design was replaced by the larger throat area, 60 deg relative exit angle, brake presented in this paper. This brake was designed to work with the test turbine facility specified in Tables 1 and 2. The blade shape is shown in Fig. 2 and brake details are given in Table 3.

Before manufacturing a full size turbobrake, it was felt wise to validate the design by testing a scale model at representative nondimensional operating conditions.

Model Scaling

In both a full size and a model turbobrake, the mass flow rate, $\dot{m}$, total temperature, T_{01}, turbobrake mean blade speed, U, and downstream pressure, p_2, are set. The test gas used determines viscosity, μ_{01}, gas constant, R, and ratio of specific heats, γ. These independent variables determine the power, P, and upstream total pressure, p_{01}, the dependent variables, for a given run. So,

$$P, p_{01} = f(\dot{m}, T_{01}, U, p_2, \mu_{01}, R, \gamma, D).$$

There are thus nine interrelated variables in each case and four primary physical quantities (i.e., mass, length, time, and temperature). Buckingham's pi theorem states that these may be reduced to relationships between $9 - 4 = 5$ nondimensional groups. These may be chosen as shown below:

$$\frac{P/\dot{m}}{U^2}, \frac{\dot{m}\sqrt{(RT_{01})}}{p_{01} D^2} = f\left(\frac{U}{\sqrt{(\gamma R T_{01})}}, \frac{p_{01}}{p_2}, \frac{\dot{m}}{\mu_{01} D}, \gamma\right)$$

or

$$\psi, \phi = f\left(\frac{U}{a_{01}}, \frac{p_{01}}{p_2}, \mathrm{Re}, \gamma\right)$$

where ϕ is the flow coefficient.

In the model tests described below, all the above parameters were correctly modeled apart from p_{01}/p_2, which was kept sufficiently high to choke the blade passages.

Model Test Facility

Commercial air motors (Tech Developments Inc. Model 51H) were found to provide a quick and inexpensive basis for a 0.17 scale model turbobrake transient test facility. As shown in Fig. 4, the turbine on the first motor is replaced by a model flow straightener and turbobrake rotor. The model turbobrake rotor, shown in Fig. 5, was machined from aluminum alloy as a blisk with integral blades. A coupled second air motor is used to drive the turbobrake up to test speed. A flow of test gas through the turbobrake is then very rapidly turned on, and the angular deceleration measured.

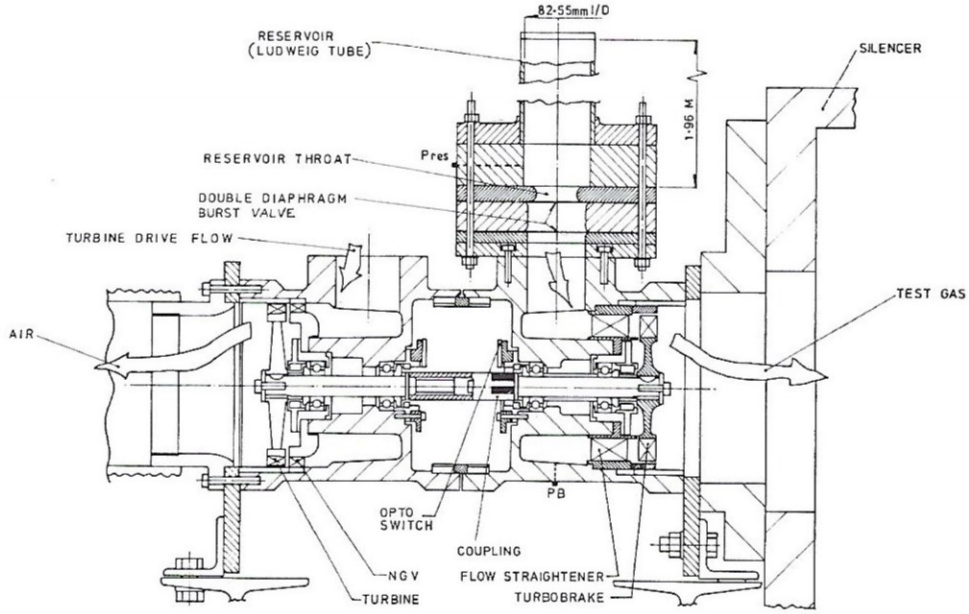

Fig. 4 Model (0.17 scale) axial turbobrake test facility, constructed from two modified air motors mounted back to back

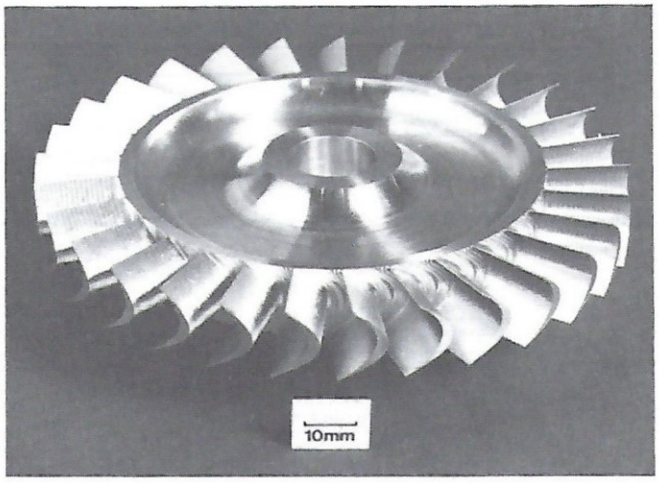

Fig. 5 Photograph of 0.17 scale test axial turbobrake rotor

Immediately before the run all the power of the driving air motor is used to overcome friction in the bearings and carbon-faced seals as well as the turbobrake windage. So, on releasing the test gas, vitually all the power developed *initially* by the turbobrake is used to decelerate the rotating components (provided the turbobrake windage, existing only before test gas release, is small). Therefore, $P = I\,\dot{\omega}\,\omega$, giving stage loading

$$\psi = \frac{I\,\dot{\omega}\,\omega}{\dot{m}\,U^2}.$$

Thus, the angular deceleration $\dot{\omega}$ is a direct measure of stage loading. The total moment of inertia of the rotating components, I, was measured using the tri-filar suspension technique and found to be only 1.6 percent less than that calculated from the design.

To model the higher speeds, it is necessary to use a 54.5 percent carbon-dioxide and 45.5 percent argon mixture (mole fractions) as the test gas. This has the same γ as air, with a lower speed of sound, allowing the design blade Mach number to be reached at 39,000 rpm rather than at 47,000 rpm for air, which is beyond safe operation of the air motor rotor.

A Ludweig Tube (Ludweig, 1957) is used as the test gas reservoir. This simple device supplies the turbobrake with gas at a constant mass flow rate and total temperature during the run. A double diaphragm was burst to start the run, and the mass flow was metered by a choked throat. The 1.96-m-long, 82.55-mm-i.d. Ludweig tube used gave a run time of 14 ms for the CO_2/Ar test gas and 11 ms for air.

For correct scaling, the model turbobrake pressures are higher than those in the ILPC. Consequently, it was possible for the model turbobrake to remain choked while exhausting it to atmospheric (room) pressure instead of a vacuum. This simplified the rig design.

Pressures were measured with SensorTechnic pressure transducers, which have a response time of 1 ms and are temperature compensated to ± 1.5 percent full scale (between 0 and 70°C). Type K thermocouples (40 μV/°C) measured temperature with a 5 ms response time. A reflective opto-switch detecting the passing of black bands painted on the coupling between the air motors gave angular displacement from which angular velocity and deceleration were found. A Datalab DL1200 transient recorder sampled at 200 kHz for 20.5 ms during a run, and the data was processed with a Matlab software package.

Test Results

Figure 6 shows typical plots of reservoir pressure, turbobrake upstream static pressure, and turbobrake speed for the 0.17 scale model at design conditions. The torque could be measured from the angular velocity curve with good repeatability.

Figure 7 shows that, as expected, the theoretical performance (Eq. (1)) of the turbobrake exceeds that required to absorb the turbine power by a considerable margin over most of the speed range. The highest experimental curve (marked full power) shows that the turbobrake *is* more powerful than the turbine over the turbine test speed range (1.40 times at design speed).

Figure 7 also shows the experimental turbobrake stage loading is in surprisingly close agreement with the simple two-dimensional theory in Eq. (1). Some of the 12 percent shortfall will be due to separations and three-dimensional effects and to the 7 percent tip leakage area between the blade and the shroud. Turbobrake windage, which exits only before test gas release, will also reduce the measured values at high speeds.

Control System

The turbobrake power has to be reduced to match the turbine

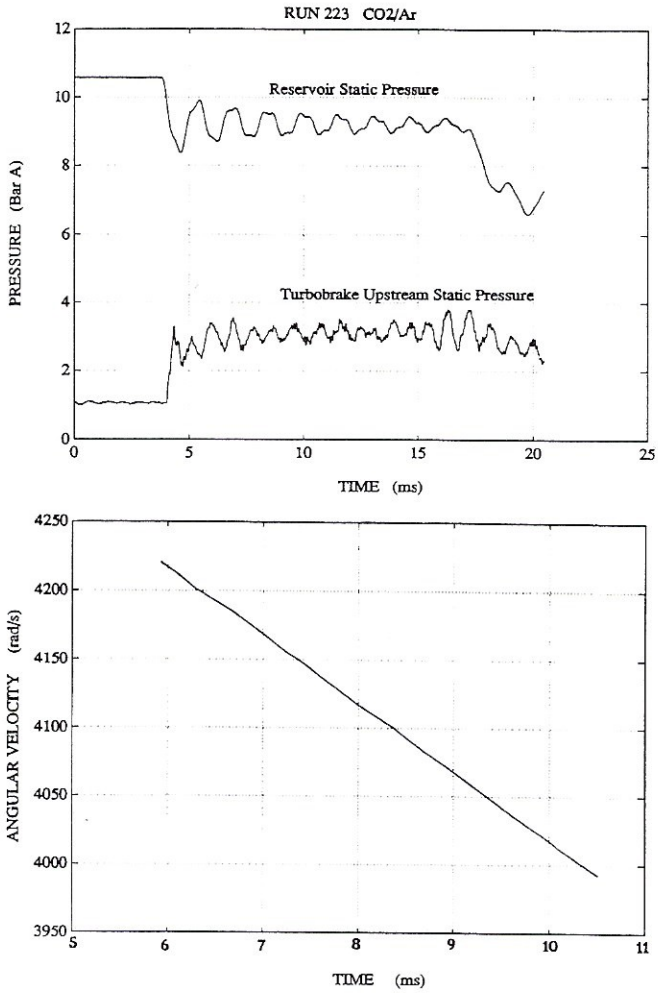

Fig. 6 Typical traces of reservoir static pressure, turbobrake upstream static pressure, and turbobrake shaft angular velocity from a 0.17 scale model test at design conditions. The Ludweig tube gives a steady flow from about 4 ms to 17 ms.

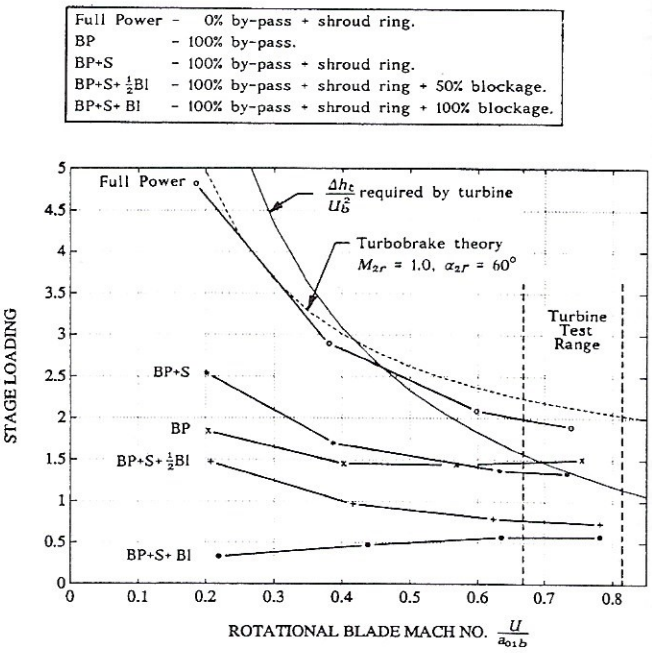

Fig. 7 Predicted and measured stage loadings for 0.17 scale model axial turbobrake. The effects of a range of control settings are shown.

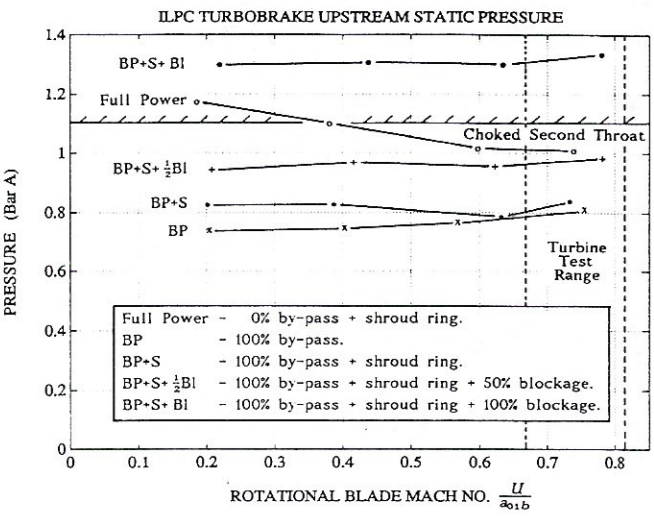

Fig. 8 Full-scale axial turbobrake upstream static pressures obtained by rescaling values measured on 0.17 scale model. The effects of a range of control settings are shown.

power to give a constant speed run. Variable inlet guide vanes were rejected as the possible control range is inadequate and the mechanical complexity high.

The simplest method of control is to bypass mass flow around the turbobrake: Since $P = \dot{m}\,\psi\,U^2$, reducing $\dot{m}$ reduces P. Initial schemes used annular plates forming a shroud around the turbobrake blades, which could be moved radially outward to allow a percentage of the mass flow to leak over the blade tips. In Fig. 7, the curve marked *BP* shows this system to work well at low speeds, but inadequately at higher speeds. The large radial pressure gradient in the swirling exit flow together with flow centrifuged from the blade tips are thought to be responsible.

A second control system (Fig. 1) was tested with a shroud ring to separate the blade tips from the bypass flow. To reduce the turbobrake mass flow further, blockage rings of different internal diameter can be bolted to it to partially block the blade exit flow. Shortened annular plates set the bypass flow over the shroud to allow fine power adjustment.

The results from the model tests in Fig. 7 show this approach to be successful, giving a wide range of controllable turbobrake power. Note that the turbobrake still absorbs power with 100 percent downstream blockage because of leakage around the rings and possible reverse flow at the leading edge tips.

On the basis of these successful model tests, it is intended to use this control system on the full size turbobrake.

The turbobrake power increases, relative to the turbine power, with speed. Once matched, the turbine-turbobrake assembly will maintain itself at a stable, constant speed without the need for a fast-acting control system.

The Second Throat

For the second throat (Fig. 1) to remain choked, and thus aerodynamically isolate the test turbine from turbobrake, its downstream static pressure must be below 1.11 bar at design. The throat downstream static pressure is the same as that upstream of the turbobrake, which is set by the turbobrake throat area.

The static pressure upstream of the model turbobrake was measured and scaled down to that of the full-size ILPC turbobrake, using the fact that the flow coefficient, $\phi = \dot{m}\sqrt{(RT_{01})}/[p_{01}\,D]$ is the same. The results shown in Fig. 8 show that the pressures are below 1.11 bar except in the extreme, and not relevant, cases of 100 percent downstream blockage or very low speed.

Thus the turbobrake can operate over the turbine test speed range without unchoking the isolating throat.

Future Developments

Following the success of these tests, a full-size turbobrake is now under manufacture and will be installed as part of the new rotating turbine section in the Isentropic Light Piston Cascade at the Royal Aerospace Establishment at Pyestock, England.

Providing the exit pressure can be kept sufficiently low, the model tests have shown that the axial turbobrake could also be used as a brake for a continuously running turbine facility. The only additions required would be simple, lossy, downstream vanes in the exit duct to absorb the high degree of swirl generated. This swirl is not a problem in short duration facilities, as it is dissipated slowly in the dump tank after the run.

Conclusions

A new single-stage turbomachine, the axial turbobrake, has been developed. It can more than absorb the power of the first stage of a large modern transonic gas turbine. A simple two-dimensional theory can be used to predict its performance with surprising accuracy. Model tests have demonstrated that it operates as predicted and that the power absorbed can be controlled over a large range by a combination of flow bypass and downstream blockage. Although initially developed for use on short-duration facilities, the turbobrake is also applicable to continuously running facilities.

Acknowledgments

Thanks are due to the Royal Aerospace Establishment, Pyestock, for their support of this work. Thanks are also due to the late Professor Don Schultz for his work on the design of the ILPC, to Gareth Horton at RAE for his design work on both blade profiles, to the Osney Lab. technicians, including Bob Taylor who machined the blade profiles, and to Richard Harris and his team at Foxley Design Associates Ltd.

References

Ainsworth, R. W., Schultz, D. L., Davies, M. R. D., Forth, C. J. P., Hilditch, M. A., Oldfield, M. L. G., and Sheard, A. G., 1988, "A Transient Flow Facility for the Study of Thermofluid-Dynamics of a Full Stage Turbine Under Engine Representative Conditions," ASME Paper No. 88-GT-144.

Brooks, A. J., Colbourne, D. E., Wedlake, E. T., Jones, T. V., Oldfield, M. L. G., Schultz, D. L., and Loftus, P. J., 1985, "The Isentropic Light Piston Annular Cascade Facility at RAE Pyestock," AGARD CP-390, pp. 31.1–31.23.

Dunn, M. G., Rae, W. J., and Holt, J. L., 1984, "Measurement and Analysis of Heat Flux Data in a Turbine Stage: Part I—Description of Experimental Apparatus and Data Analysis," ASME *Journal of Engineering for Gas Turbines and Power*, Vol. 106, pp. 229–233.

Epstein, A. H., Guenette, G. R., and Norton, R. J. G., 1984, "The MIT Blowdown Turbine Facility," ASME Paper No. 84-GT-116.

Epstein, A. H., Guenette, G. R., and Norton, R. J. G., 1985, "The Design of the MIT Blowdown Turbine Facility," MIT Gas Turbine Lab. Report No. 183, Apr.

Foor, W. B., and Jansen, W., 1984, "The Application of Air Dynamometers for Testing Turbo-shaft Gas Turbine Engines," ASME Paper No. 84-GT-216.

Gosling, M. C., 1984, "The Design, Manufacture and Operation of a Model Turbine Test Rig," ASME Paper No. 84-GT-130.

Heinemann, H., 1979, "The Test Facility for Rotating Annular Cascades of the DFVLR and Its Measurement and Evaluation Method," ICIASF 79 Record, IEEE publication, New York.

Judge, A. W., 1955, *The Testing of High Speed Internal Combustion Engines*, Chapman and Hall, pp. 154–226.

Ludweig, H., 1957, "Tube Wind Tunnel, a Special Type of Blowdown Tunnel," AGARD Report 143, July.

Schultz, D. L., 1983, "A Study of the Feasibility of Installing a Rotor in the R.A.E. Pyestock Free Piston Cascade," Internal Report.